

Elastic and transition form factors of light pseudoscalar mesons from QCD sum rules

Irina Balakireva¹, Wolfgang Lucha², and Dmitri Melikhov^{1,2,3}

¹*SINP, Moscow State University, 119991, Moscow, Russia*

²*HEPHY, Austrian Academy of Sciences, Nikolsdorfergasse 18, A-1050, Vienna, Austria*

³*Faculty of Physics, University of Vienna, Boltzmannngasse 5, A-1090, Vienna, Austria*

(Dated: June 28, 2018)

We revisit $F_\pi(Q^2)$ and $F_{P\gamma}(Q^2)$, $P = \pi, \eta, \eta'$, making use of the local-duality (LD) version of QCD sum rules. We give arguments, that the LD sum rule provides reliable predictions for these form factors at $Q^2 \geq 5 - 6 \text{ GeV}^2$, the accuracy of the method increasing with Q^2 in this region. For the pion elastic form factor, the well-measured data at small Q^2 give a hint that the LD limit may be reached already at relatively low values of momentum transfers, $Q^2 \approx 4 - 8 \text{ GeV}^2$; we therefore conclude that large deviations from LD in the region $Q^2 = 20 - 50 \text{ GeV}^2$ seem very unlikely. The data on the $(\eta, \eta') \rightarrow \gamma\gamma^*$ form factors meet the expectations from the LD model. However, the BABAR results for the $\pi^0 \rightarrow \gamma\gamma^*$ form factor imply a violation of LD growing with Q^2 even at $Q^2 \approx 40 \text{ GeV}^2$, at odds with the η, η' case and with the general properties expected for the LD sum rule.

PACS numbers: 11.55.Hx, 12.38.Lg, 03.65.Ge, 14.40.Be

1. INTRODUCTION

In spite of the long history of theoretical investigations of the pion, its properties are still not fully understood.

At asymptotically large values of the momentum transfer, $Q^2 \rightarrow \infty$, the pion elastic and the $\pi\gamma$ transition form factors obey perturbative QCD (pQCD) factorization theorems [1, 2]

$$F_\pi(Q^2) \rightarrow 8\pi\alpha_s(Q^2)f_\pi^2/Q^2, \quad F_{\pi\gamma}(Q^2) \rightarrow \sqrt{2}f_\pi/Q^2, \quad f_\pi = 130 \text{ MeV}. \quad (1.1)$$

Subleading logarithmic and power corrections modify the behaviour (1.1) at large but finite Q^2 .

In early applications of QCD to the pion elastic form factor, $F_\pi(Q^2)$, one hoped that power corrections vanish rather fast with Q^2 ; however, later investigations revealed that nonperturbative power corrections dominate the form factor $F_\pi(Q^2)$ up to relatively high $Q^2 \approx 10 - 20 \text{ GeV}^2$. This picture has arisen from different approaches [3–8]. It was found that even at Q^2 as large as $Q^2 = 20 \text{ GeV}^2$ the $O(1)$ term provides about half of the form factor; the pQCD formula based on factorization starts to work well only at $Q^2 \geq 50 - 100 \text{ GeV}^2$.

For the pion-photon transition form factor, $F_{\pi\gamma}(Q^2)$, axial anomaly [9, 10] fixes its value at $Q^2 = 0$. Brodsky and Lepage proposed a simple interpolating formula between the known value of the form factor at $Q^2 = 0$ and its asymptotic behaviour (1.1)

$$F_{\pi\gamma}(Q^2) = \frac{1}{2\sqrt{2}\pi^2 f_\pi} \left(1 + \frac{Q^2}{4\pi^2 f_\pi^2}\right)^{-1}, \quad (1.2)$$

which was believed to describe well the transition form factor in a broad range of Q^2 .

Surprisingly, some of the recent studies of the pion elastic form factor in the region $Q^2 \approx 5 - 50 \text{ GeV}^2$ [11–14] reported much larger value of the pion elastic form factor than expected before (see Fig. 1); the BABAR result on the $\pi \rightarrow \gamma\gamma^*$ transition form factor [16] imply a strong violation of pQCD factorization in the region of Q^2 up to 40 GeV^2 .

In this paper, we revisit $F_\pi(Q^2)$ and $F_{P\gamma}(Q^2)$ making use of the local-duality (LD) version [17, 18] of QCD sum rules [19]. Our main emphasis is on the analysis of the expected accuracy of this powerful (although approximate) method for the calculation of hadron form factors.

A local-duality sum rule is a dispersive three-point sum rule at $\tau = 0$ (i.e., infinitely large Borel mass parameter). In this case all power corrections vanish and all details of the non-perturbative dynamics are hidden in one quantity – the Q^2 -dependent effective continuum threshold. Implementing duality in the standard way, i.e., as the low-energy cut in the dispersion representations for the form factors, the sum rules relate the pion form factors to the low-energy region of Feynman diagrams of pQCD:

$$F_\pi^{\text{LD}}(Q^2) = \frac{1}{f_\pi^2} \int_0^{s_{\text{eff}}(Q^2)} ds_1 \int_0^{s_{\text{eff}}(Q^2)} ds_2 \Delta_{\text{pert}}(s_1, s_2, Q^2), \quad F_{\pi\gamma}^{\text{LD}}(Q^2) = \frac{1}{f_\pi} \int_0^{\bar{s}_{\text{eff}}(Q^2)} ds \sigma_{\text{pert}}(s, Q^2). \quad (1.3)$$

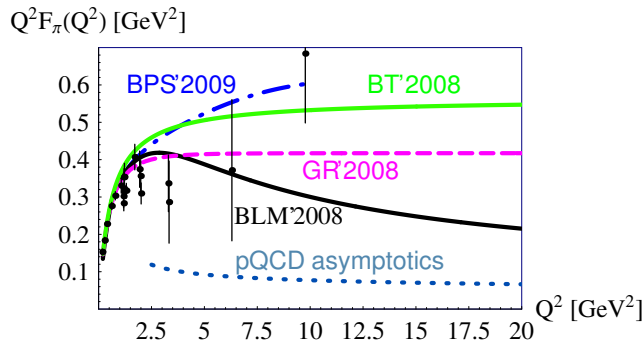


Fig. 1: Some predictions for the pion elastic form factor $F_\pi(Q^2)$ — lower solid (black) line: BLM'2008 [8], upper solid (green) line: BT'2008 [11], dashed (magenta) line: GR'2008 [12], and dash-dotted (blue) line: BPS'2009 [14, Eq. (4.11b)] — vs. experiment [15].

Here $\Delta_{\text{pert}}(s_1, s_2, Q^2)$ is the double spectral density of the $\langle AVA \rangle$ 3-point function; whereas $\sigma_{\text{pert}}(s, Q^2)$ is the single spectral density of the $\langle AVV \rangle$ 3-point function. These quantities are calculated as power series in α_s :

$$\Delta_{\text{pert}}(s_1, s_2, Q^2) = \Delta_{\text{pert}}^{(0)}(s_1, s_2, Q^2) + \alpha_s \Delta_{\text{pert}}^{(1)}(s_1, s_2, Q^2) + O(\alpha_s^2), \quad \sigma_{\text{pert}}(s, Q^2) = \sigma_{\text{pert}}^{(0)}(s, Q^2) + O(\alpha_s^2). \quad (1.4)$$

The one-loop spectral densities $\Delta_{\text{pert}}^{(0)}$ and $\sigma_{\text{pert}}^{(0)}$ are well-known [20–22]. The two-loop contribution $\Delta_{\text{pert}}^{(1)}$ has been calculated in [23]; the two-loop $O(\alpha_s)$ correction to σ_{pert} was found to be zero [24]. Higher-order radiative corrections are unknown.

If one knows the effective thresholds $s_{\text{eff}}(Q^2)$ and $\bar{s}_{\text{eff}}(Q^2)$, Eqs. (1.3) provide the form factors. However, finding a reliable criterion for fixing the thresholds is a very subtle and difficult problem investigated in great detail in [25].

Due to specific properties of the spectral functions at large values of the momentum transfer, the LD form factors (1.3) obey the factorization theorems (1.1) as soon as the effective thresholds satisfy the following relations:

$$s_{\text{eff}}(Q^2 \rightarrow \infty) = \bar{s}_{\text{eff}}(Q^2 \rightarrow \infty) = 4\pi^2 f_\pi^2. \quad (1.5)$$

For finite Q^2 , however, the effective thresholds $s_{\text{eff}}(Q^2)$ and $\bar{s}_{\text{eff}}(Q^2)$ depend on Q^2 and differ from each other [26]. The “conventional LD model” arises if one assumes (1.5) for all “not too small” values of Q^2 [17]:

$$s_{\text{eff}}(Q^2) = \bar{s}_{\text{eff}}(Q^2) = 4\pi^2 f_\pi^2. \quad (1.6)$$

Obviously, the LD model (1.6) for the effective continuum thresholds is an approximation which does not take into account details of the confinement dynamics. The only property of theory relevant for this model is factorization of hard form factors at large values of the momentum transfers. Because of the approximate character of the predictions from LD sum rules, it is important to understand the expected accuracy of the form factors obtained by this method. Quantum-mechanical potential models provide a possibility to probe this accuracy: one calculates the exact form factors by making use of the solutions of the Schrödinger equation and confronts these results with the application of LD sum rules in quantum mechanics [27–29].

This paper is organized as follows: In the next section, we recall details of LD sum rules in QCD and of the LD model for form factors. Section 3 studies the accuracy of the LD model for elastic and transition form factors in a quantum-mechanical potential model. The pion elastic form factor is discussed in Section 4 and the $P \rightarrow \gamma\gamma^*$ transition form factors are considered in Section 5. Section 6 gives our conclusions. Appendix A provides technical details of perturbative two-loop calculations in non-relativistic field theory.

2. LOCAL-DUALITY MODEL FOR FORM FACTORS IN QCD

The sum-rule calculations of the hadron form factors are based on the OPE for the relevant correlation functions, which contain the contributions of ground-state hadrons of interest. In order to extract the form factors of pseudoscalar mesons, one analyses the $\langle AVA \rangle$ and $\langle AVV \rangle$ correlators, A being the axial and V the vector currents.

A. The three-point function $\langle AVA \rangle$ and the pion elastic form factor

The basic objects for the extraction of the pion decay constant and the elastic form factor are the two- and three-point correlation functions

$$\begin{aligned}\Pi(p^2) &= \int d^4x e^{ipx} \langle 0 | T[j(x) j^\dagger(0)] | 0 \rangle, \\ \Gamma(p_1^2, p_2^2, q^2) &= \int d^4x_1 d^4x_2 e^{i(p_1x_1 - p_2x_2)} \langle 0 | T[j(x_1) J(0) j^\dagger(x_2)] | 0 \rangle, \quad q \equiv p_1 - p_2, \quad Q^2 \equiv -q^2;\end{aligned}\quad (2.1)$$

where $|0\rangle$ is the physical QCD vacuum, which differs from pQCD vacuum; properties of the physical QCD vacuum are characterized by the condensates [19]. j is shorthand for the interpolating axial current $j_{5\alpha}$ of the positively charged pion,

$$\langle 0 | j_{5\alpha}(0) | \pi(p) \rangle = ip_\alpha f_\pi. \quad (2.2)$$

J labels the electromagnetic current J_μ , and for brevity we omit all Lorentz indices. In QCD, the correlators (2.1) can be found by applying OPE. Instead of discussing the Green functions (2.1) in Minkowski space, it is convenient to study the time-evolution operators in Euclidean space, which arise upon performing the Borel transformation $p^2 \rightarrow \tau$ to a parameter τ related to Euclidean time. The Borel image of the two-point correlator $\Pi(p^2)$ is

$$\Pi_{\text{OPE}}(\tau) = \int_0^\infty ds e^{-s\tau} \rho_{\text{pert}}(s) + \Pi_{\text{cond}}(\tau), \quad \rho_{\text{pert}}(s) = \rho_0(s) + \alpha_s \rho_1(s) + O(\alpha_s^2), \quad (2.3)$$

with spectral densities $\rho_i(s)$ related to perturbative two-point graphs, and nonperturbative power corrections $\Pi_{\text{cond}}(\tau)$. At hadron level, insertion of intermediate hadron states casts the Borel-transformed two-point correlator into the form

$$\Pi(\tau) = f_\pi^2 e^{-m_\pi^2 \tau} + \text{excited states}. \quad (2.4)$$

In this expression for $\Pi(\tau)$, the first term on the right-hand side constitutes the pion contribution. Applying the double Borel transform $p_{1,2}^2 \rightarrow \tau/2$ to the three-point correlator $\Gamma(p_1^2, p_2^2, q^2)$ results, at QCD level, in

$$\begin{aligned}\Gamma_{\text{OPE}}(\tau, Q^2) &= \int_0^\infty \int_0^\infty ds_1 ds_2 \exp\left(-\frac{s_1 + s_2}{2} \tau\right) \Delta_{\text{pert}}(s_1, s_2, Q^2) + \Gamma_{\text{cond}}(\tau, Q^2), \\ \Delta_{\text{pert}}(s_1, s_2, Q^2) &= \Delta_0(s_1, s_2, Q^2) + \alpha_s \Delta_1(s_1, s_2, Q^2) + O(\alpha_s^2),\end{aligned}\quad (2.5)$$

where $\Delta_{\text{pert}}(s_1, s_2, Q^2)$ is the double spectral density of the three-point graphs of perturbation theory and $\Gamma_{\text{cond}}(\tau, Q^2)$ labels the power corrections. Inserting intermediate hadron states yields, for the hadron-level expression for $\Gamma(\tau, Q^2)$,

$$\Gamma(\tau, Q^2) = F_\pi(Q^2) f_\pi^2 e^{-m_\pi^2 \tau} + \text{excited states}. \quad (2.6)$$

Quark-hadron duality assumes that above effective continuum thresholds s_{eff} the excited-state contributions are dual to the high-energy regions of the perturbative graphs. In this case, the relevant sum rules read in the chiral limit [17, 30]

$$\begin{aligned}f_\pi^2 &= \int_0^{\bar{s}_{\text{eff}}(\tau)} ds e^{-s\tau} \rho_{\text{pert}}(s) + \frac{\langle \alpha_s G^2 \rangle}{12\pi} \tau + \frac{176\pi \alpha_s \langle \bar{q}q \rangle^2}{81} \tau^2 + \dots, \\ F_\pi(Q^2) f_\pi^2 &= \int_0^{s_{\text{eff}}(Q^2, \tau)} \int_0^{s_{\text{eff}}(Q^2, \tau)} ds_1 ds_2 \Delta_{\text{pert}}(s_1, s_2, Q^2) \exp\left(-\frac{s_1 + s_2}{2} \tau\right) \\ &\quad + \frac{\langle \alpha_s G^2 \rangle}{24\pi} \tau + \frac{4\pi \alpha_s \langle \bar{q}q \rangle^2}{81} \tau^2 (13 + Q^2 \tau) + \dots.\end{aligned}\quad (2.7)$$

As a consequence of the use of local condensates, the right-hand side of (2.8) involves polynomials in Q^2 and therefore increases with Q^2 , whereas the form factor $F_\pi(Q^2)$ on the left-hand side should decrease with Q^2 . Hence, at large Q^2

the sum rule (2.8), with its truncated series of power corrections, cannot be directly used. There are essentially two ways for considering the region of large Q^2 .

One remedy is the resummation of power corrections: the resummed power corrections decrease with increasing Q^2 . This may be achieved by the introduction of nonlocal condensates [31] in a, however, model-dependent manner [32].

Another option is to fix the Borel parameter τ to the value $\tau = 0$, thus arriving at a local-duality sum rule [17, 18]. Therein all power corrections vanish and the remaining perturbative term decreases with Q^2 . In the LD limit, one finds

$$f_\pi^2 = \int_0^{\tilde{s}_{\text{eff}}} ds \rho_{\text{pert}}(s) = \frac{\tilde{s}_{\text{eff}}}{4\pi^2} \left(1 + \frac{\alpha_s}{\pi}\right) + O(\alpha_s^2), \quad (2.9)$$

$$F_\pi(Q^2) f_\pi^2 = \int_0^{s_{\text{eff}}(Q^2)} \int_0^{s_{\text{eff}}(Q^2)} ds_1 ds_2 \Delta_{\text{pert}}(s_1, s_2, Q^2). \quad (2.10)$$

The spectral densities $\rho_{\text{pert}}(s)$ and $\Delta_{\text{pert}}(s_1, s_2, Q^2)$ are calculable by perturbation theory. Hence, by fixing \tilde{s}_{eff} and $s_{\text{eff}}(Q^2)$, it is straightforward to extract the pion's decay constant f_π and form factor $F_\pi(Q^2)$.

Noteworthy, the effective and the physical thresholds are different quantities: The latter is a constant determined by the masses of the hadron states. The effective thresholds \tilde{s}_{eff} and s_{eff} are parameters of the sum-rule method related to the specific realization of quark–hadron duality; in general, they are *not* constant but depend on external kinematical variables [25, 26].

Let us recall the important properties of the spectral densities on the right-hand sides of (2.3) and (2.5): For $Q^2 \rightarrow 0$, the Ward identity relates the spectral densities $\rho_i(s)$ and $\Delta_i(s_1, s_2, Q^2)$ of two- and three-point functions to each other:

$$\lim_{Q^2 \rightarrow 0} \Delta_i(s_1, s_2, Q^2) = \rho_i(s_1) \delta(s_1 - s_2), \quad i = 0, 1, \dots \quad (2.11)$$

For $Q^2 \rightarrow \infty$ and $s_{1,2}$ kept fixed, explicit calculations [8] yield

$$\lim_{Q^2 \rightarrow \infty} \Delta_0(s_1, s_2, Q^2) \propto \frac{1}{Q^4}, \quad \lim_{Q^2 \rightarrow \infty} \Delta_1(s_1, s_2, Q^2) = \frac{8\pi}{Q^2} \rho_0(s_1) \rho_0(s_2). \quad (2.12)$$

For the pion form factor $F_\pi(Q^2)$ on the left-hand side of (2.8) two exact properties are known, namely, its normalization condition related to current conservation, requiring $F_\pi(0) = 1$, and the factorization theorem (1.1). Obviously, for

$$s_{\text{eff}}(Q^2 \rightarrow 0) = \frac{4\pi^2 f_\pi^2}{1 + \alpha_s(0)/\pi}, \quad s_{\text{eff}}(Q^2 \rightarrow \infty) = s_{\text{LD}} \equiv 4\pi^2 f_\pi^2, \quad (2.13)$$

the form factor $F_\pi(Q^2)$ extracted from the LD sum rule (2.10) satisfies both of these rigorous constraints. At small Q^2 , we assume a freezing of $\alpha_s(Q^2)$ at the level 0.3, as is frequently done. At the intermediate Q^2 , the effective threshold depends on Q^2 and the pion form factor obtained from the LD sum rule depends on the details of $s_{\text{eff}}(Q^2)$. The “conventional LD model” *assumes* that reasonable predictions for the elastic form factor at not too small values of Q^2 may be obtained by setting $s_{\text{eff}}(Q^2) = 4\pi^2 f_\pi^2$, see Eq. (1.6).

Although one has to invoke assumptions on behaviour of the effective threshold at the intermediate Q^2 , some features of the pion form factor turn out to be largely independent of this assumption. So, let us look more carefully what is in fact conjectured in the LD sum rule and what may be predicted by this approach.

The sum rule (2.10) for the pion form factor relies on two ingredients: first, on the *rigorous calculation* of the spectral densities of the perturbative-QCD diagrams (recall that power corrections vanish in the LD limit $\tau = 0$); second, on the *assumption* of quark–hadron duality, which claims that the contributions of the hadronic continuum states may be well described by the diagrams of perturbation theory above some effective threshold s_{eff} . Thus, the only — although really essential — unknown ingredient of the LD sum rule for the pion elastic form factor is this effective continuum threshold $s_{\text{eff}}(Q^2)$. Let us emphasize that, since the $O(1)$ and $O(\alpha_s)$ contributions to the pion form factor are governed by one and the same effective threshold $s_{\text{eff}}(Q^2)$, the relative weights of these contributions may be *predicted*. Their ratio $F_\pi^{(0)}(Q^2)/F_\pi^{(1)}(Q^2)$ turns out to be relatively stable with respect to s_{eff} and may therefore be calculated relatively accurately (see Fig. 2).

Quark–hadron duality implies that the effective threshold (although being a function of Q^2) always — i.e., also for large Q^2 — stays in a region close to 1 GeV². Moreover, in order to satisfy the QCD factorization theorem for the $O(\alpha_s)$ contribution to the form factor, the effective threshold should behave like $s_{\text{eff}}(Q^2) \rightarrow 4\pi^2 f_\pi^2$ for $Q^2 \rightarrow \infty$. This requirement has immediate consequences for the large- Q^2 behaviour of different contributions to the pion form factor:

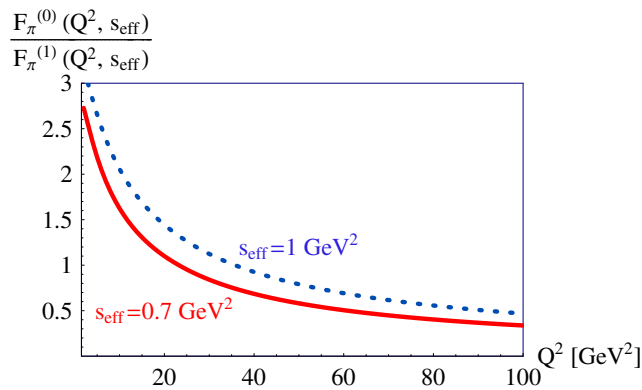


Fig. 2: Ratio $F_\pi^{(0)}(Q^2)/F_\pi^{(1)}(Q^2)$ of $O(1)$ and $O(\alpha_s)$ contributions to the pion elastic form factor vs. Q^2 for two reasonable values of the — here by assumption constant — effective threshold s_{eff} .

1. Since $s_{\text{eff}}(Q^2)$ is bounded from above, the $O(1)$ contribution $F_\pi^{(0)}(Q^2)$ to the elastic form factor $F_\pi(Q^2)$ of the pion behaves like $F_\pi^{(0)}(Q^2) \propto 1/Q^4$ for $Q^2 \rightarrow \infty$. We would like to emphasize that the decrease of the soft contribution to the pion elastic form factor like $1/Q^4$ is a direct consequence of perturbation theory and quark–hadron duality.

2. Consequently, for large Q^2 the pion elastic form factor $F_\pi(Q^2)$ is dominated by the $O(\alpha_s)$ contribution $F_\pi^{(1)}(Q^2)$. Now, in the holographic models of [11, 12] merely the soft contribution is considered: it behaves like $1/Q^2$ for large Q^2 . This is only possible if the effective threshold $s_{\text{eff}}(Q^2)$ rises with Q^2 . However, this immediately leads to the violation of the factorization theorem for the $O(\alpha_s)$ contribution, which is governed by the same effective threshold. Consequently, we would like to emphasize that the findings of [11, 12] would imply that the QCD factorization theorem is violated. We thus conclude that the predictions of [11, 12] for the pion form factor seem to us improbable.¹

B. The three-point function $\langle VAV \rangle$ and the $P \rightarrow \gamma$ transition form factor

Let us now consider the amplitude of two-photon production from the vacuum induced by the axial-vector current of nearly massless quarks of one flavour, $j_\mu^5 = \bar{q}\gamma_\mu\gamma_5q$, with $\varepsilon_{1,2}$ denoting the photon polarization vectors:

$$\langle \gamma(q_1)\gamma(q_2) | j_\mu^5(x=0) | 0 \rangle = T_{\mu\alpha\beta}(p|q_1, q_2) \varepsilon_1^\alpha \varepsilon_2^\beta, \quad p = q_1 + q_2. \quad (2.14)$$

The amplitude $T_{\mu\alpha\beta}$ is obtained from the vacuum expectation value of the T -product of two vector and one axial-vector currents and will be referred to as the $\langle VAV \rangle$ amplitude. Vector-current conservation yields the following relations:

$$T_{\mu\alpha\beta}(p|q_1, q_2)q_1^\alpha = 0, \quad T_{\mu\alpha\beta}(p|q_1, q_2)q_2^\beta = 0. \quad (2.15)$$

The general decomposition of the amplitude may be written as

$$T_{\mu\alpha\beta}(p|q_1, q_2) = -p_\mu \epsilon_{\alpha\beta q_1 q_2} iF_0 + (q_1^2 \epsilon_{\mu\alpha\beta q_2} - q_{1\alpha} \epsilon_{\mu q_1 \beta q_2}) iF_1 + (q_2^2 \epsilon_{\mu\beta\alpha q_1} - q_{2\beta} \epsilon_{\mu q_2 \alpha q_1}) iF_2. \quad (2.16)$$

The form factor F_0 contains the contribution of the pseudoscalar meson of our interest [33] such that

$$F_{P \rightarrow \gamma\gamma}(q_1^2, q_2^2) = -\frac{1}{f_P} F_0(p^2 = m_P^2 | q_1^2, q_2^2). \quad (2.17)$$

We also consider the transition amplitude of the pseudoscalar current operator $\bar{q}\gamma_5q$:

$$\langle \gamma(q_1)\gamma(q_2) | \bar{q}\gamma_5q | 0 \rangle = \epsilon_{\alpha\beta q_1 q_2} \varepsilon_1^\alpha \varepsilon_2^\beta F_5(q_1^2, q_2^2, p^2). \quad (2.18)$$

¹ A way out would be to assume different effective thresholds for the $O(1)$ and the $O(\alpha_s)$ contributions to the pion form factor. This seems, however, a rather artificial construction.

The two-photon amplitude of the divergence of the axial current takes the form

$$\langle \gamma(q_1) \gamma(q_2) | \partial^\mu j_\mu^5 | 0 \rangle = \epsilon_{\alpha\beta q_1 q_2} \varepsilon_1^\alpha \varepsilon_2^\beta (p^2 F_0 - q_1^2 F_1 - q_2^2 F_2). \quad (2.19)$$

The case of our interest is $q_1^2 = 0$, then the form factor F_1 does not contribute to the divergence. In perturbation theory, the form factors F_0 , F_2 , and F_5 may be written in terms of their spectral representations in p^2 (with $q^2 \equiv q_2^2 = -Q^2$):

$$F_i(p^2, q^2) = \frac{1}{\pi} \int_{4m^2}^{\infty} \frac{ds}{s-p^2} \Delta_i(s, q^2). \quad (2.20)$$

To one-loop order, the spectral densities read [20–22]

$$\begin{aligned} \Delta_0(s, q^2) &= -\frac{1}{2\pi} \frac{1}{(s-q^2)^2} \left[-q^2 w + 2m^2 \log\left(\frac{1+w}{1-w}\right) \right], \\ \Delta_2(s, q^2) &= -\frac{1}{2\pi} \frac{1}{(s-q^2)^2} \left[-s w + 2m^2 \log\left(\frac{1+w}{1-w}\right) \right], \\ \Delta_5(s, q^2) &= -\frac{1}{2\pi} \frac{m}{s-q^2} \log\left(\frac{1+w}{1-w}\right), \quad w \equiv \sqrt{1-4m^2/s}. \end{aligned} \quad (2.21)$$

Obviously, the absorptive parts Δ_i obey the classical equation of motion for the divergence of the axial current

$$s \Delta_0(s, q^2) - q^2 \Delta_2(s, q^2) = 2m \Delta_5(s, q^2). \quad (2.22)$$

The form factors then satisfy

$$p^2 F_0(p^2, q^2) - q^2 F_2(p^2, q^2) = 2m F_5(p^2, q^2) - \frac{1}{\pi} \int_{4m^2}^{\infty} ds \Delta_0(s, q^2). \quad (2.23)$$

The last integral is equal to $-1/2\pi$, independently of the values of m and q^2 , and represents the axial anomaly [9]:

$$p^2 F_0(p^2, q^2) - q^2 F_2(p^2, q^2) = 2m F_5(p^2, q^2) + \frac{1}{2\pi^2}. \quad (2.24)$$

In the chiral limit $m = 0$ and for $q^2 = 0$, the form factor F_0 develops a pole related to a massless pseudoscalar meson [34]. The residue of this pole is again the axial-anomaly $1/2\pi^2$. Notice however that the pole in the one-loop expression for F_0 disappears as soon as one of the photons is virtual [20, 34, 35].

As is clear from (2.23), the anomaly represents the integral of Δ_0 , the spectral density of the form factor F_0 . Adler and Bardeen [10] tell us that the anomaly is non-renormalized by multiloop corrections. The easiest realization of this property would have been just the vanishing of multiloop contributions to the spectral density $\Delta_0(s, q^2)$. An argument in favour of this possibility comes from explicit two-loop calculations [24] which report the non-renormalizability of the full $\langle VAV \rangle$ vertex to the two-loop accuracy. However, if so, the full form factor F_0 is given by its one-loop expression. Then, this expression should develop the pion pole, known to be present in the full amplitude for any value of q^2 . But, obviously, this pole does not emerge in the one-loop expression for F_0 if $q^2 \neq 0$!

This requires that multiloop corrections to the form factor F_0 (and, respectively, to its absorptive part $\Delta_0(s, q^2)$) do not vanish. Then one may ask oneself how it may happen that the anomaly nevertheless remains non-renormalized by multiloop corrections? The only possible answer we see [33] is that the non-renormalization of the anomaly is reached due to some conspiral property of multiloop contributions to $\Delta_0(s, q^2)$ forcing their integral to vanish (in fact, quite similar to the one-loop result: although the spectral density explicitly depends on m and q^2 , its integral is an m - and q^2 -independent constant).

As is obvious from (2.16), the contribution of the light pseudoscalar constitutes a part of the form factor F_0 . The Borel sum rule for the corresponding Lorentz structure reads ($Q^2 = -q^2 > 0$)

$$\int ds \exp(-s\tau) \Delta_0(s, Q^2) = -f_P F_{P\gamma}(Q^2) \exp(-m_P^2 \tau) + \text{contributions of excited states}. \quad (2.25)$$

Exploiting the concept of duality, the contribution of the excited states is assumed to be dual to the high-energy region of the diagrams of perturbation theory above an effective threshold s_{eff} . After that, setting the Borel parameter $\tau = 0$

we arrive at the LD sum rule for a pseudoscalar $\bar{q}q$ -meson

$$\int_{4m^2}^{s_{\text{eff}}(Q^2)} ds \Delta_0(s, Q^2) = -f_P F_{P\gamma}(Q^2). \quad (2.26)$$

The spectral density Δ_0 to one-loop order is given by (2.21); two-loop corrections were found to be absent [24]. As discussed above, higher-loop corrections to Δ_0 cannot vanish; so the l.h.s. of (2.26) is known to $O(\alpha_s^2)$ accuracy.

In the chiral limit, the LD expression for the form factor for the one-flavour case is particularly simple (cf. [18, 42]):

$$F_{P\gamma}(Q^2) = \frac{1}{2\pi^2 f_P} \frac{s_{\text{eff}}(Q^2)}{s_{\text{eff}}(Q^2) + Q^2}. \quad (2.27)$$

We would like to emphasize that the effective threshold in (2.27) depends on Q^2 . Apart from neglecting α_s^2 and higher-order corrections to the spectral density Δ_0 , no approximations have been done up to now: we have just considered the LD limit $\tau = 0$; for an appropriate choice of $s_{\text{eff}}(Q^2)$ the form factor may still be calculated exactly. Approximations come into the game when we consider a model for $s_{\text{eff}}(Q^2)$.

Independently of the behaviour of $s_{\text{eff}}(Q^2)$, the form factor at $Q^2 = 0$ is related to the axial anomaly: $F_{P\gamma}(0) = 1/(2\pi^2 f_P)$. QCD factorization requires $s_{\text{eff}}(Q^2) \rightarrow 4\pi^2 f_P^2$ for large Q^2 . So, the simplest model compatible with this requirement is obtained by setting $s_{\text{eff}}(Q^2) = 4\pi^2 f_P^2$ for *all* values of Q^2 [17]. This is the ‘‘conventional LD model’’ (1.6) yielding for the neutral pion case the Brodsky–Lepage interpolating formula 1.2.²

As already pointed out above, the conventional LD model for the effective continuum threshold (1.6), defined by the choice $s_{\text{eff}}(Q^2) = \bar{s}_{\text{eff}}(Q^2) = 4\pi^2 f_\pi^2$ for all Q^2 , or a slightly more sophisticated approach of [8] are approximations which do not account for subtle details of the confinement dynamics. Consequently, it is important to understand the accuracy to be expected within this approach; in other words, it is important to obtain some reliable estimate of the expected deviations of the exact $s_{\text{eff}}(Q^2)$ from its LD limit s_{LD} in the momentum region $Q^2 \geq 4\text{--}6 \text{ GeV}^2$. To this end, in the next Section we take advantage of the fact that in quantum mechanics all the bound-state properties may be found exactly by solving the Schrödinger equation. On the other hand, also in quantum mechanics we may construct LD sum rules.

3. EXACT VS. LD FORM FACTORS IN QUANTUM-MECHANICAL POTENTIAL MODELS

The relevance and the expected accuracy of the LD model may be tested in those cases where the form factor $F_{P\gamma}(Q^2)$ is known, i.e., may be calculated by other theoretical approaches or measured experimentally. Then, the exact effective threshold may be reconstructed from (2.27), in this way probing the accuracy of the LD model.

To probe the accuracy of the LD model, we now consider a quantum-mechanical example: the corresponding form factors may be calculated using the solution of the Schrödinger equation and confronted with the results of the quantum-mechanical LD model, which is constructed precisely the same way as in QCD. For the elastic form factor, it is mandatory to consider a potential involving both the Coulomb and the confining parts; for the analysis of the transition form factor one may start with a purely confining potential.

The basic object for quantum-mechanical LD sum rules is the analogue of the three-point correlator of field theory [26]

$$\Gamma^{\text{NR}}(E, E', Q) = \langle r' = 0 | \frac{1}{H - E'} J(\mathbf{q}) \frac{1}{H - E} | r = 0 \rangle, \quad Q \equiv |\mathbf{q}|. \quad (3.1)$$

Here, H is the Hamiltonian of the model; the current operator $J(\mathbf{q})$ is determined by its kernel $\langle \mathbf{r}' | J(\mathbf{q}) | \mathbf{r} \rangle = \exp(i\mathbf{q} \cdot \mathbf{r}) \delta^{(3)}(\mathbf{r} - \mathbf{r}')$. We do not take the spin of the current into account, therefore the basic quantum-mechanical Green function is the same for both types of form factors discussed above.

² In an alternative approach to the $P\gamma$ form factor [36, 37], the pseudoscalar meson is described by a set of distribution amplitudes of increasing twist which are treated as nonperturbative inputs. In our analysis, the deviation of the effective threshold $s_{\text{eff}}(Q^2)$ from its asymptotic value $4\pi^2 f_P^2$ corresponds to some extent to the contribution of higher-twist distribution amplitudes in the approach of [37].

A. Elastic form factor

The elastic form factor of the ground state is given in terms of its wave function Ψ by

$$F_{\text{el}}(Q) = \langle \Psi | J(\mathbf{q}) | \Psi \rangle = \int d^3r \exp(i\mathbf{q} \cdot \mathbf{r}) |\Psi(\mathbf{r})|^2 = \int d^3k \Psi(\mathbf{k}) \Psi(\mathbf{k} + \mathbf{q}), \quad Q \equiv |\mathbf{q}|. \quad (3.2)$$

Here, Ψ is the ground state of the Hamiltonian

$$H = \frac{\mathbf{k}^2}{2m} - \frac{\alpha}{r} + V_{\text{conf}}(r), \quad r \equiv |\mathbf{r}|. \quad (3.3)$$

Because of the presence of the Coulomb interaction in the potential, the asymptotic behaviour of the form factor at large values of Q is given by the factorization theorem [38]

$$F_{\text{el}}(Q) \xrightarrow{Q \rightarrow \infty} \frac{16\pi \alpha m R_g}{Q^4}, \quad R_g \equiv |\Psi(\mathbf{r} = \mathbf{0})|^2. \quad (3.4)$$

The quantum-mechanical LD sum rule for the form factor $F_{\text{el}}(Q)$ is rather similar to that in QCD: The double Borel transform ($E \rightarrow T$, $E' \rightarrow T'$) of (3.1) may be written in the form

$$\Gamma^{\text{NR}}(T, T', Q) = \int dk' \exp\left(-\frac{k'^2 T'}{2m}\right) \int dk \exp\left(-\frac{k^2 T}{2m}\right) \Delta_{\text{pert}}^{\text{NR}}(k, k', Q) + \Gamma_{\text{power}}^{\text{NR}}(T, T', Q), \quad (3.5)$$

where $\Gamma_{\text{power}}^{\text{NR}}(T, T', Q)$ describes the contribution of the confining interaction and $\Delta_{\text{pert}}^{\text{NR}}(k, k', Q)$ is the double spectral density of Feynman diagrams of nonrelativistic perturbation theory, see Appendix A for details.

Setting $T' = T = 0$ leads to the LD sum rule, in which case $\Gamma_{\text{power}}^{\text{NR}}$ vanishes [25]. The low-energy region of perturbative diagrams—below some effective continuum threshold $k_{\text{eff}}(Q)$ —is assumed to be dual to the ground-state contribution, which reads $R_g F_{\text{el}}(Q^2)$. Finally, we arrive at the following LD expression for the elastic form factor:

$$R_g = \int_0^{k_{\text{eff}}} dk \rho_{\text{pert}}^{\text{QM}}(k) = \frac{k_{\text{eff}}^3}{6\pi^2} + \alpha m \frac{k_{\text{eff}}^2}{9\pi} + O(\alpha^2), \quad (3.6)$$

$$F_{\text{el}}^{\text{LD}}(Q) = \frac{1}{R_g} \int_0^{k_{\text{eff}}(Q)} dk \int_0^{k_{\text{eff}}(Q)} dk' \Delta_{\text{pert}}^{\text{QM}}(k, k', Q). \quad (3.7)$$

The explicit result for $\Delta_{\text{pert}}^{\text{QM}}(k_1, k_2, Q)$ is given in Appendix A.

The factorization formula (3.4) is reproduced by the LD sum rule (3.7) if the momentum-dependent effective threshold behaves as

$$k_{\text{eff}}(Q) \xrightarrow{Q \rightarrow \infty} k_{\text{LD}} \equiv (6\pi^2 R_g)^{1/3}. \quad (3.8)$$

B. Transition form factor

The analogue of the $\pi\gamma$ transition form factor in quantum mechanics is given by

$$F_{\text{trans}}(Q, E) = \langle \Psi | J(\mathbf{q}) \frac{1}{H - E} | r = 0 \rangle, \quad (3.9)$$

The case of one real and one virtual photon corresponds to $E = 0$ and $Q \neq 0$. At large Q , the transition form factor $F_{\text{trans}}(Q) \equiv F_{\text{trans}}(Q, E = 0)$ satisfies the factorization theorem

$$F_{\text{trans}}(Q) \xrightarrow{Q \rightarrow \infty} \frac{2m\sqrt{R_g}}{Q^2}. \quad (3.10)$$

Recall that the behaviour (3.10) does not require the Coulomb potential in the interaction and—in distinction to the factorization of the elastic form factor—emerges also for a purely confining interaction.

The LD sum rule for the form factor $F_{\text{trans}}(Q)$ is constructed on the basis of the same three-point function (3.1) and has the form

$$F_{\text{trans}}^{\text{LD}}(Q) = \frac{1}{\sqrt{R_g}} \int_0^{\bar{k}_{\text{eff}}(Q)} dk \int_0^\infty dk' \Delta_{\text{pert}}^{\text{QM}}(k, k', Q). \quad (3.11)$$

Notice that the k' -integration is not restricted to the low-energy region since we do not isolate the ground-state contribution in the initial state. The asymptotical behaviour (3.10) is correctly reproduced by Eq. (3.11) for

$$\bar{k}_{\text{eff}}(Q \rightarrow \infty) = k_{\text{LD}}. \quad (3.12)$$

C. Quantum-mechanical LD model

As is obvious from (3.8) and (3.12), the effective thresholds for the elastic and for the transition form factors have the same limit at large Q :

$$k_{\text{eff}}(Q \rightarrow \infty) = \bar{k}_{\text{eff}}(Q \rightarrow \infty) = k_{\text{LD}}. \quad (3.13)$$

The LD model emerges when one *assumes* that also for intermediate Q one may find a reasonable estimate for the form factors by setting

$$k_{\text{eff}}(Q) = \bar{k}_{\text{eff}}(Q) = k_{\text{LD}}. \quad (3.14)$$

Similarly to QCD, the only property of the bound state which determines the form factor in the LD model is R_g .

D. LD vs. exact effective threshold

Let us now calculate the exact thresholds $k_{\text{eff}}(Q)$ and $\bar{k}_{\text{eff}}(Q)$ which reproduce the exact form factor by the LD expression; they are obtained by solving the LD sum rules (3.7) and (3.11) using the exact form factors on the left-hand sides of these equations. The deviation of the LD threshold k_{LD} from these exact thresholds measures the error induced by the approximation (3.14) and characterizes the accuracy of the LD model.

For our numerical analysis we use parameter values relevant for hadron physics: $m = 0.175$ GeV for the reduced constituent light-quark mass and $\alpha = 0.3$. We considered several confining potentials

$$V_{\text{conf}}(r) = \sigma_n (m r)^n, \quad n = 2, 1, 1/2, \quad (3.15)$$

and adapt the strengths σ_n in our confining interactions such that the Schrödinger equation yields for each potential the same value of the wave function at the origin, $\Psi(r=0) = 0.078$ GeV^{3/2}, which holds for $\sigma_2 = 0.71$ GeV, $\sigma_1 = 0.96$ GeV, and $\sigma_{1/2} = 1.4$ GeV. The ground state then has a typical hadron size ~ 1 fm.

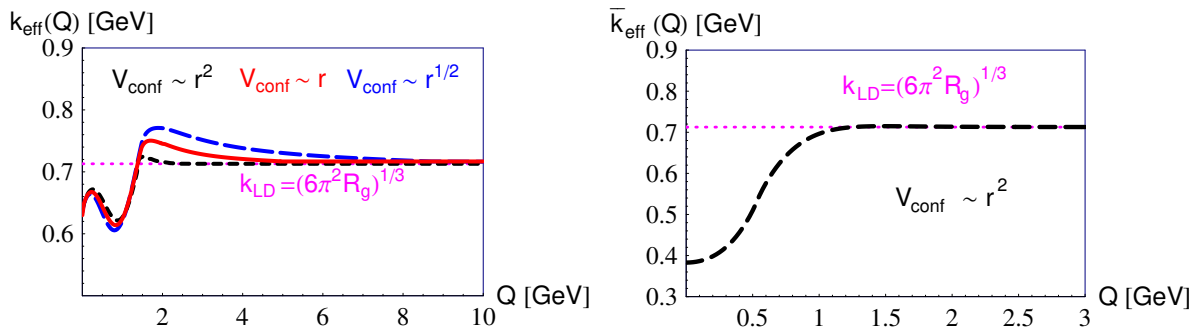


Fig. 3: Exact effective thresholds in quantum mechanics for the elastic (left) and the transition (right) form factors for different confining potentials. $R_g \equiv |\Psi(r=0)|^2$.

Figure 3 presents the exact effective thresholds. Independently of the details of the confining interaction, the accuracy of the LD approximation for the effective threshold and, respectively, the accuracy of the LD elastic form factor increases with Q in the region $Q^2 \geq 5 - 8$ GeV². For the transition form factor, the LD approximation works well starting with even smaller values of Q .

4. THE PION ELASTIC FORM FACTOR

The $O(1)$ and $O(\alpha_s)$ spectral densities are at our disposal, and the only missing ingredient for obtaining the form factor is s_{eff} . We know the rigorous constraints on the effective threshold—at $Q^2 = 0$ from the Ward identity and at $Q^2 \rightarrow \infty$ from factorization—so it is easy to construct a model for $s_{\text{eff}}(Q^2)$ by a smooth interpolation between these values. A simple parameterization with a single constant Q_0 fixed by fitting the data at $Q^2 = 1 \text{ GeV}^2$ might read [39]

$$s_{\text{eff}}(Q^2) = \frac{4\pi^2 f_\pi^2}{1 + \alpha_s(0)/\pi} \left[1 + \tanh\left(\frac{Q^2}{Q_0^2}\right) \frac{\alpha_s(0)}{\pi} \right], \quad Q_0^2 = 2.02 \text{ GeV}^2. \quad (4.1)$$

According to Fig. 1, our interpolation perfectly describes the well-measured data in the range $Q^2 \approx 0.5\text{--}2.5 \text{ GeV}^2$.

Note that the effective continuum threshold $s_{\text{eff}}(Q^2)$ in Eq. (4.1) approaches its limit s_{LD} already at $Q^2 \approx 4\text{--}5 \text{ GeV}^2$. For $Q^2 > 4\text{--}5 \text{ GeV}^2$, it practically coincides with the LD effective threshold of [17]. Moreover, for $Q^2 > 5\text{--}6 \text{ GeV}^2$ the formula (4.1) is pretty close to the model of [8]. Obviously, the model labeled BLM in Fig. 1 provides a perfect description of the available $F_\pi(Q^2)$ data in the region $Q^2 = 1\text{--}2.5 \text{ GeV}^2$. For $Q^2 \geq 3\text{--}4 \text{ GeV}^2$, it reproduces well all the data, except for a point at $Q^2 = 10 \text{ GeV}^2$, where it is off the present experimental value, which anyhow has a rather large error, by some two standard deviations.³

Interestingly, in the region $Q^2 \geq 3\text{--}4 \text{ GeV}^2$ the BLM model yields considerably lower predictions than the results of the different theoretical approaches presented in Refs. [11–14].

For a given result for the pion form factor, we define the *equivalent effective threshold* as the quantity which reproduces this result by Eq. (1.3). Figure 4 displays the equivalent effective thresholds recalculated from the data and from the theoretical predictions for the elastic form factor from Fig. 1. For the $F_\pi(Q^2)$ predictions of [11, 12, 14], the corresponding equivalent effective thresholds $s_{\text{eff}}(Q^2)$ recalculated from (2.10) are depicted in Fig. 4: In all cases, they considerably exceed, for larger Q^2 , the LD limit s_{LD} dictated by factorization. Moreover, their deviation from s_{LD} increases with Q^2 .

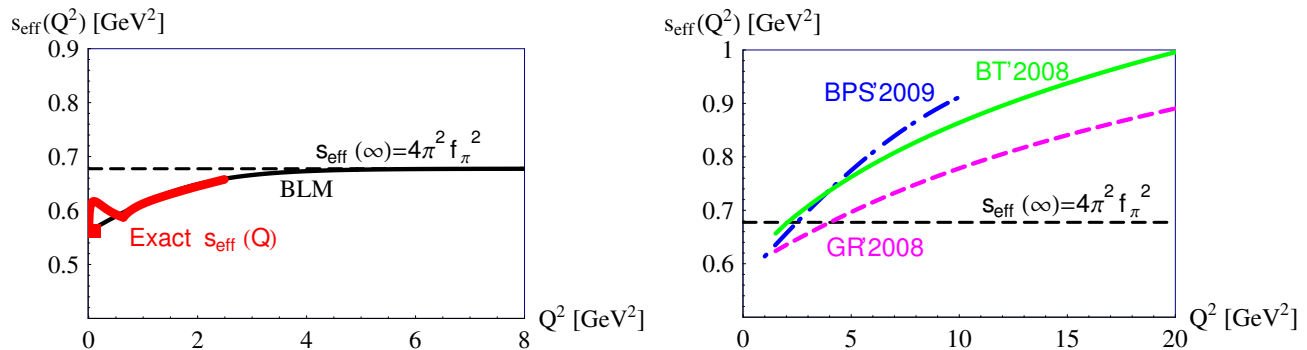


Fig. 4: Left: the “equivalent effective threshold” extracted from the data (red) vs. the improved LD model (BLM) of [39]. Right: equivalent thresholds for the theoretical predictions displayed in Fig. 1.

The exact effective threshold extracted from the accurate data at low Q^2 suggests that the LD limit may be reached already at relatively low values of $Q^2 \approx 4\text{--}8 \text{ GeV}^2$. However, the results in the right plot imply that the accuracy of the LD model still does not increase—or even decreases—with Q^2 even in the region $Q^2 \simeq 20 \text{ GeV}^2$, in conflict with both our experience from quantum mechanics and the hint from the data at low Q^2 . We look forward to the future accurate data expected from JLab in the range up to $Q^2 = 8 \text{ GeV}^2$.

³ It is virtually impossible to construct models compatible with all experimental results within $Q^2 = 2.5\text{--}10 \text{ GeV}^2$, as revealed by closer inspection of Fig. 1: those approaches which hit the data at $Q^2 = 10 \text{ GeV}^2$ overestimate the better-quality data points at $Q^2 \approx 2\text{--}4 \text{ GeV}^2$.

5. THE (π^0, η, η') $\rightarrow \gamma\gamma^*$ TRANSITION FORM FACTORS

A. $(\eta, \eta') \rightarrow \gamma\gamma^*$

Before discussing the π^0 case, let us consider the η and η' decays. Here, one has to take properly into account the $\eta - \eta'$ mixing and the presence of two—strange and nonstrange—LD form factors. Following [5, 40, 41] we describe the flavor structure of η and η' as⁴

$$|\eta\rangle = \left| \frac{\bar{u}u + \bar{d}d}{\sqrt{2}} \right\rangle \cos \phi - |\bar{s}s\rangle \sin \phi, \quad |\eta'\rangle = \left| \frac{\bar{u}u + \bar{d}d}{\sqrt{2}} \right\rangle \sin \phi + |\bar{s}s\rangle \cos \phi, \quad \phi \approx 39.3^\circ. \quad (5.1)$$

The η and η' form factors then take the form

$$F_{\eta\gamma}(Q^2) = \frac{5}{3\sqrt{2}} F_{n\gamma}(Q^2) \cos \phi - \frac{1}{3} F_{s\gamma}(Q^2) \sin \phi, \quad F_{\eta'\gamma}(Q^2) = \frac{5}{3\sqrt{2}} F_{n\gamma}(Q^2) \sin \phi + \frac{1}{3} F_{s\gamma}(Q^2) \cos \phi. \quad (5.2)$$

Here, $F_{n\gamma}(Q^2)$ and $F_{s\gamma}(Q^2)$ are the form factors describing the transition of the nonstrange and $\bar{s}s$ -components, respectively. The LD expressions for these quantities read

$$F_{n\gamma}(Q^2) = \frac{1}{f_n} \int_0^{s_{\text{eff}}^{(n)}(Q^2)} ds \sigma_{\text{pert}}^{(n)}(s, Q^2), \quad F_{s\gamma}(Q^2) = \frac{1}{f_s} \int_{4m_s^2}^{s_{\text{eff}}^{(s)}(Q^2)} ds \sigma_{\text{pert}}^{(s)}(s, Q^2), \quad (5.3)$$

where $\sigma_{\text{pert}}^{(n)}$ and $\sigma_{\text{pert}}^{(s)}$ denote σ_{pert} with the corresponding quark propagating in the loop. Let us mention that for an isosinglet axial-vector current, a QCD axial anomaly contributes to the amplitude of interest [43] and to the spectral densities of the form factors. This effect is of the order α_s^2 and is not expected to be important at large Q^2 . An overall agreement of the form factor from the LD model for η and η' mesons with the data speaks in favour of this expectation.

In numerical calculations we set $m_u = m_d = 0$ and $m_s = 100$ MeV. The LD model involves two separate effective thresholds for the nonstrange and the strange components [40]:

$$s_{\text{eff}}^{(n)} = 4\pi^2 f_n^2, \quad f_n \approx 1.07 f_\pi, \quad s_{\text{eff}}^{(s)} = 4\pi^2 f_s^2, \quad f_s \approx 1.36 f_\pi. \quad (5.4)$$

According to the experience from quantum mechanics, the LD model may not perform well for small values of Q^2 , where the true effective threshold is smaller than the LD threshold; however, for larger Q^2 the LD model in quantum mechanics gives accurate predictions for the form factors, as illustrated by Fig. 4. Figure 5 shows the corresponding

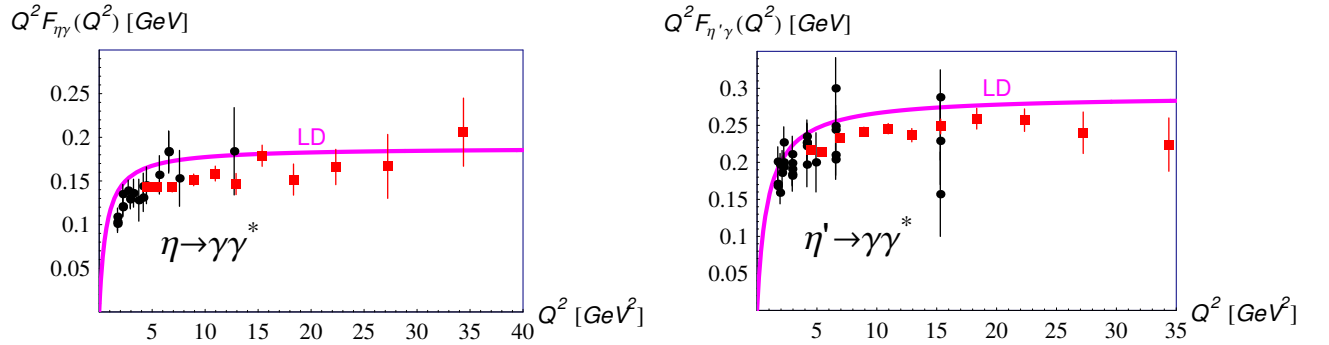


Fig. 5: LD predictions for η and η' vs. experimental data from [44] (black) and [45] (red).

predictions for η and η' mesons. One observes an overall agreement between the LD model and the data, meeting the expectation from quantum mechanics.

⁴ For comparison with the form factors obtained in a scheme based on the octet–singlet mixing, we refer to [42].

B. $\pi^0 \rightarrow \gamma\gamma^*$

Surprisingly, for the pion transition form factor, Fig. 6, one observes a clear disagreement between the results from the LD model and the BABAR data [16]. Moreover—in evident conflict with the η and η' results and the experience from quantum mechanics—the data implies that the violations of LD increase with Q^2 even in the region $Q^2 \approx 40 \text{ GeV}^2$! The effective threshold extracted from the BABAR data is compatible with a linear growing function of Q^2 with no sign of approaching the LD limit.

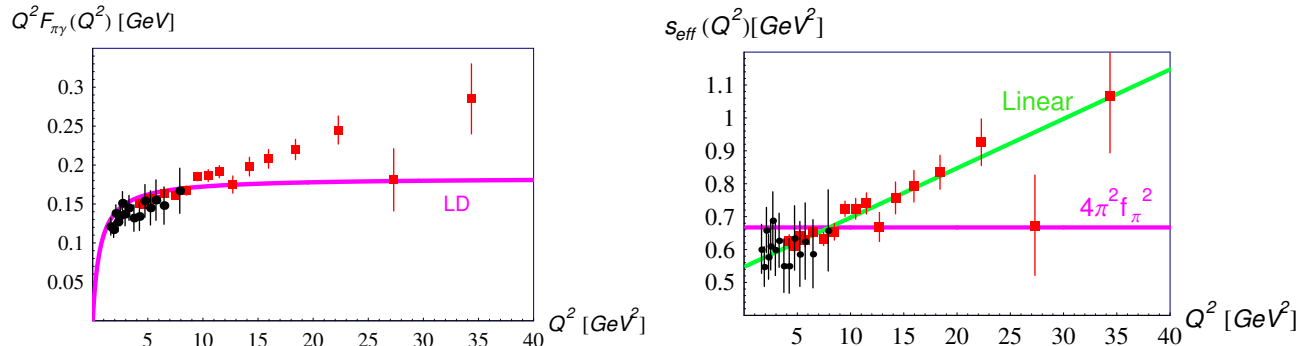


Fig. 6: The LD $\pi\gamma$ form factor vs. data from [44] (black) and [16] (red) and the corresponding equivalent effective threshold.

The $P \rightarrow \gamma$ transition form factors have been addressed recently in many publications (see, e.g., [36, 37, 42, 46–54]). However, no convincing explanation of the full picture of the $P \rightarrow \gamma$ transition form factors has been offered. In fact, it is hard to find a convincing answer to the question why nonstrange components in η , η' , on the one hand, and in π^0 , on the other hand, should behave so much differently?

6. SUMMARY

We presented the analysis of the pion elastic and the π^0 , η , η' transition form factors from the LD version of QCD sum rules. The main emphasis was laid on the attempt to probe the accuracy of this approximate method and the reliability of its predictions. Our main conclusions are as follows:

- **The elastic form factor:** Our quantum-mechanical analysis suggests that the LD model should work increasingly well in the region $Q^2 \geq 4 - 8 \text{ GeV}^2$, independently of the details of the confining interaction. For arbitrary confining interaction, the LD model gives very accurate results for $Q^2 \geq 20 - 30 \text{ GeV}^2$. The accurate data on the pion form factor at small momentum transfers indicate that the LD limit for the effective threshold, $s_{\text{eff}}^{\text{LD}} = 4\pi^2 f_\pi^2$, may be reached already at relatively low values $Q^2 = 5 - 6 \text{ GeV}^2$; thus, large deviations from the LD limit at $Q^2 = 20 - 50 \text{ GeV}^2$ reported in some recent publications [11–14] appear to us rather unlikely.
- **The $P \rightarrow \gamma\gamma^*$ transition form factor:** We conclude from the quantum-mechanical analysis that the LD model should work well in the region $Q^2 \geq$ a few GeV^2 . Indeed, for the $\eta \rightarrow \gamma\gamma^*$ and $\eta' \rightarrow \gamma\gamma^*$ form factors, the predictions from LD model in QCD work reasonably well. Surprisingly, for the $\pi \rightarrow \gamma\gamma^*$ form factor the present BABAR data indicate an increasing violation of local duality, corresponding to a linearly rising effective threshold, even at Q^2 as large as 40 GeV^2 . This puzzle has so far no compelling theoretical explanation. Our conclusion agrees with the findings of [37, 46, 47] obtained from other theoretical approaches.

Acknowledgments. We are grateful to S. Mikhailov, O. Nachtmann, S. Simula, O. Teryaev, and particularly to B. Stech for valuable discussions. D. M. was supported by the Austrian Science Fund (FWF) under Project No. P22843. This work was supported in part by grants for leading scientific schools 1456.2008.2 and 3920.2012.2, and by FASI State Contract No. 02.740.11.0244.

Appendix A: Perturbative expansion of Green functions in quantum mechanics

We construct the perturbative expansions of both polarization operator and vertex function in quantum mechanics.

1. Polarization operator

The polarization operator $\Pi(E)$ is defined by [27]

$$\Pi(E) = \langle \mathbf{r}' = \mathbf{0} | G(E) | \mathbf{r} = \mathbf{0} \rangle, \quad (\text{A.1})$$

where $G(E)$ is the full Green function, i.e., $G(E) = (H - E)^{-1}$, defined by the model Hamiltonian under consideration

$$H = H_0 + V(r), \quad H_0 \equiv \frac{\mathbf{k}^2}{2m}, \quad r \equiv |\mathbf{r}|. \quad (\text{A.2})$$

The expansion of the full Green function $G(E)$ in powers of the interaction potential V has the well-known form

$$G(E) = G_0(E) - G_0(E)V G_0(E) + G_0(E)V G_0(E)V G_0(E) + \dots, \quad (\text{A.3})$$

with $G_0(E) = (H_0 - E)^{-1}$. It generates the corresponding expansion of $\Pi(E)$:

$$\Pi(E) = \Pi_0(E) + \Pi_1(E) + \dots. \quad (\text{A.4})$$

Explicitly, one finds

$$\Pi_0(E) = \frac{1}{(2\pi)^3} \int \frac{d^3k}{\frac{\mathbf{k}^2}{2m} - E}, \quad (\text{A.5})$$

$$\Pi_1(E) = -\frac{1}{(2\pi)^6} \int \frac{d^3k}{\frac{\mathbf{k}^2}{2m} - E} \frac{d^3k'}{\frac{\mathbf{k}'^2}{2m} - E} V((\mathbf{k} - \mathbf{k}')^2). \quad (\text{A.6})$$

We consider interaction potentials $V(r)$ which consist of a Coulombic and a confining part:

$$V(r) = -\frac{\alpha}{r} + V_{\text{conf}}(r). \quad (\text{A.7})$$

Then the expansion (A.4) becomes a double expansion in powers of the Coulomb coupling α and the confining potential V_{conf} (see Fig. 7).

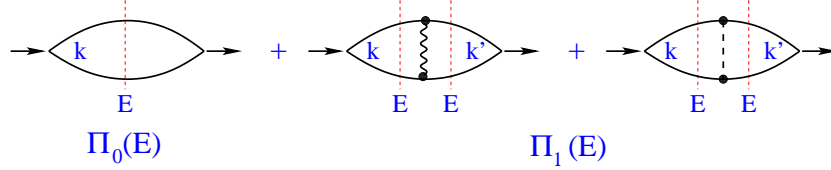


Fig. 7: Expansion of the polarization operator in terms of Coulomb (wavy line) and confining (dashed line) interaction potentials.

The contribution to $\Pi(E)$ arising from the Coulombic potential is referred to as the perturbative contribution, Π_{pert} . The contributions involving the confining potential V_{conf} (including the mixed terms receiving contributions from both confining and Coulomb parts) are referred to as the power corrections, Π_{power} . For instance, the first-order perturbative contribution reads

$$\Pi_1^{(\alpha)}(E) = \frac{1}{(2\pi)^6} \int \frac{d^3k}{\frac{\mathbf{k}^2}{2m} - E} \frac{d^3k'}{\frac{\mathbf{k}'^2}{2m} - E} \frac{4\pi\alpha}{(\mathbf{k} - \mathbf{k}')^2} = \frac{\alpha m}{8\pi^2} \int \frac{d^3k}{(\frac{\mathbf{k}^2}{2m} - E) |\mathbf{k}|}. \quad (\text{A.8})$$

The integral diverges but becomes convergent after applying the Borel transformation $1/(a - E) \rightarrow \exp(-aT)$.⁵ The Borel-transformed polarization operator $\Pi(T)$ has the form [55]

$$\Pi(T) = \Pi_{\text{pert}}(T) + \Pi_{\text{power}}(T), \quad \Pi_{\text{pert}}(T) = \left(\frac{m}{2\pi T} \right)^{3/2} \left[1 + \sqrt{2\pi m T} \alpha + \frac{1}{3} m \pi^2 T \alpha^2 + O(\alpha^3) \right]. \quad (\text{A.9})$$

⁵ Note that the Borel transform of the Green function $(H - E)^{-1}$ yields the quantum-mechanical time-evolution operator in imaginary time $U(T) = \exp(-HT)$.

In the LD limit, that is, for $T \rightarrow 0$, only $\Pi_{\text{pert}}(T)$ will be relevant. Nevertheless, as an illustration we provide also the result for the power corrections $\Pi_{\text{power}}(T)$ for the case of a harmonic-oscillator confining potential $V_{\text{conf}}(r) = m\omega^2 r^2/2$:

$$\Pi_{\text{power}}(T) = \left(\frac{m}{2\pi T}\right)^{3/2} \left[-\frac{1}{4}\omega^2 T^2 \left(1 + \frac{11}{12}\sqrt{2\pi m T} \alpha\right) + \frac{19}{480}\omega^4 T^4 \right]. \quad (\text{A.10})$$

Let us point out that $\Pi_{\text{power}}(T=0)$ vanishes, similar to QCD. The radiative corrections in $\Pi_{\text{pert}}(T)$ have a less singular behaviour compared to the free Green function, so the system behaves as quasi-free system. In QCD such a behaviour, frequently regarded as an indication of asymptotic freedom, occurs due to the running of the strong coupling α_s and its vanishing at small distances. Interestingly, in the nonrelativistic potential model this feature is built-in automatically.

Now, according to the standard procedures of the method of sum rules, the dual correlator is obtained by applying a low-energy cut at some threshold \bar{k}_{eff} in the spectral representation for the perturbative contribution to the correlator:

$$\Pi_{\text{dual}}(T, \bar{k}_{\text{eff}}) = \frac{1}{2\pi^2} \int_0^{\bar{k}_{\text{eff}}} dk k^2 \exp\left(-\frac{k^2}{2m}T\right) \left[1 + \frac{\pi m \alpha}{k} + \frac{(\pi m \alpha)^2}{3k^2} + O(\alpha^3)\right] + \Pi_{\text{power}}(T). \quad (\text{A.11})$$

By construction, the dual correlator $\Pi_{\text{dual}}(T, \bar{k}_{\text{eff}})$ is related to the ground-state contribution by

$$\Pi_{\text{dual}}(T, \bar{k}_{\text{eff}}) = \Pi_{\text{g}}(T) \equiv R_{\text{g}} \exp(-E_{\text{g}}T), \quad R_{\text{g}} \equiv |\psi_{\text{g}}(r=0)|^2. \quad (\text{A.12})$$

As we have shown in our previous studies of potential models, the effective continuum threshold defined according to (A.12) is a function of the Borel time parameter T . For $T=0$, one finds

$$\Pi_{\text{dual}}(\bar{k}_{\text{eff}}, T=0) = \frac{1}{6\pi^2} \bar{k}_{\text{eff}}^3 + \frac{\alpha m}{4\pi} \bar{k}_{\text{eff}}^2 + \dots. \quad (\text{A.13})$$

2. Vertex function

We now calculate the vertex function $\Gamma(E, E', Q)$, defined by

$$\Gamma(E, E', Q) = \langle \mathbf{r}' = \mathbf{0} | G(E) J(\mathbf{q}) G(E') | \mathbf{r} = \mathbf{0} \rangle, \quad Q \equiv |\mathbf{q}|, \quad (\text{A.14})$$

where $J(\mathbf{q})$ is the operator which adds a momentum \mathbf{q} to the interacting constituent. The expansions (A.3) of the full Green functions $G(E)$ and $G(E')$ in powers of the interaction entail a corresponding expansion of $\Gamma(E, E', Q)$, cf. Fig. 8:

$$\Gamma(E, E', Q) = \Gamma_0(E, E', Q) + \Gamma_1(E, E', Q) + \dots. \quad (\text{A.15})$$

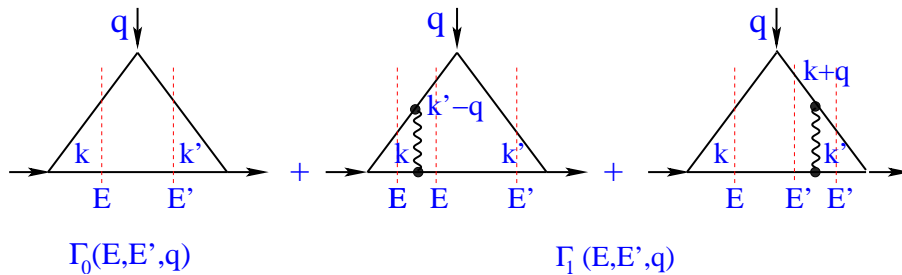


Fig. 8: Nonrelativistic Feynman diagrams representing the lowest perturbative contributions to the vertex function $\Gamma(E, E', Q)$.

For the vertex functions $\Gamma_i(E, E', Q)$, $i = 0, 1, \dots$, in (A.15), their double spectral representations may be written as

$$\Gamma_i(E, E', Q) = \int \frac{dz}{\frac{z}{2m} - E} \frac{dz'}{\frac{z'}{2m} - E'} \Delta_i(z, z', Q). \quad (\text{A.16})$$

The vertex functions $\Gamma_i(E, E', Q=0)$ and the polarization operators $\Pi_i(E)$ satisfy the Ward identities

$$\Gamma_i(E, E', Q=0) = \frac{\Pi_i(E) - \Pi_i(E')}{E - E'}, \quad (\text{A.17})$$

which are equivalent to the following relations between the corresponding spectral densities:

$$\lim_{Q \rightarrow 0} \Delta_i(z, z', Q) = \delta(z - z') \rho_i(z). \quad (\text{A.18})$$

We shall consider the double Borel transform $E \rightarrow T$ and $E' \rightarrow T'$: $(a - E)^{-1} \rightarrow \exp(-aT)$, $(a' - E')^{-1} \rightarrow \exp(-a'T')$. Equation (A.18) leads to the following Ward identities for the Borel images:

$$\Gamma_i(T, T', Q = 0) = \Pi_i(T + T'). \quad (\text{A.19})$$

a. One-loop contribution Γ_0 to the vertex function

The zero-order one-loop term has the form

$$\Gamma_0(E, E', Q) = \frac{1}{(2\pi)^3} \int \frac{d^3 k}{\left(\frac{\mathbf{k}^2}{2m} - E\right) \left(\frac{(\mathbf{k}+\mathbf{q})^2}{2m} - E'\right)}. \quad (\text{A.20})$$

This may be written as the double spectral representation

$$\Gamma_0(E, E', Q) = \int \frac{dz}{\frac{z}{2m} - E} \frac{dz'}{\frac{z'}{2m} - E'} \Delta_0(z, z', Q), \quad (\text{A.21})$$

where

$$\Delta_0(z, z', Q) = \frac{1}{(2\pi)^3} \int d^3 k \delta(z - \mathbf{k}^2) \delta(z' - (\mathbf{k} - \mathbf{q})^2) = \frac{1}{(2\pi)^3} \frac{\pi}{2Q} \theta((z' - z - Q^2)^2 - 4zQ^2 < 0). \quad (\text{A.22})$$

Hereafter, we use the notations $k \equiv \sqrt{z}$ and $k' \equiv \sqrt{z'}$. In terms of the variables k and k' , the θ function takes the form

$$\theta((z' - z - Q^2)^2 - 4zQ^2 < 0) = \theta(|k - Q| < k' < k + Q). \quad (\text{A.23})$$

b. Two-loop contribution Γ_1 to the vertex function

We consider here only corrections related to the *Coulomb* potential, since power corrections induced by the confining interaction vanish in the LD limit. The two-loop $O(\alpha)$ correction receives two contributions and has the form

$$\Gamma_1(E, E', Q) = \frac{1}{(2\pi)^6} \int \frac{d^3 k}{\frac{\mathbf{k}^2}{2m} - E} \frac{d^3 k'}{\frac{\mathbf{k}'^2}{2m} - E'} \frac{4\pi\alpha}{(\mathbf{k} - (\mathbf{k}' - \mathbf{q}))^2} \left[\frac{1}{\frac{(\mathbf{k}' - \mathbf{q})^2}{2m} - E'} + \frac{1}{\frac{(\mathbf{k} + \mathbf{q})^2}{2m} - E} \right]. \quad (\text{A.24})$$

Having in mind the subsequent application of a double Borel transformation in E and E' , it is convenient to represent Γ_1 as a sum of two terms, $\Gamma_1 = \Gamma_1^{(a)} + \Gamma_1^{(b)}$, with

$$\begin{aligned} \Gamma_1^{(a)}(E, E', Q) &= \frac{\alpha m}{8\pi^5} \int \frac{d^3 k'}{\left(\frac{\mathbf{k}'^2}{2m} - E'\right) \left(\frac{(\mathbf{k}' - \mathbf{q})^2}{2m} - E\right)} \int \frac{d^3 k}{(\mathbf{k} - (\mathbf{k}' - \mathbf{q}))^2 [\mathbf{k}^2 - (\mathbf{k}' - \mathbf{q})^2]} \\ &+ \frac{\alpha m}{8\pi^5} \int \frac{d^3 k}{\left(\frac{\mathbf{k}^2}{2m} - E\right) \left(\frac{(\mathbf{k} + \mathbf{q})^2}{2m} - E'\right)} \int \frac{d^3 k'}{((\mathbf{k} + \mathbf{q}) - \mathbf{k}')^2 [\mathbf{k}'^2 - (\mathbf{k} + \mathbf{q})^2]}, \\ \Gamma_1^{(b)}(E, E', Q) &= \frac{\alpha m}{8\pi^5} \int \frac{d^3 k}{\frac{\mathbf{k}^2}{2m} - E} \frac{d^3 k'}{\frac{\mathbf{k}'^2}{2m} - E'} \frac{1}{(\mathbf{k} + \mathbf{q} - \mathbf{k}')^2} \left[\frac{1}{(\mathbf{k}' - \mathbf{q})^2 - \mathbf{k}^2} + \frac{1}{(\mathbf{k} + \mathbf{q})^2 - \mathbf{k}'^2} \right]. \end{aligned} \quad (\text{A.25})$$

The double Borel transformation in $E \rightarrow T$ and $E' \rightarrow T'$ is now easily performed.

Let us start with $\Gamma_1^{(a)}$. One integration in $\Gamma_1^{(a)}$ may be performed, leading to

$$\Gamma_1^{(a)}(E, E', Q) = \frac{\alpha m}{16\pi^2} \left[\int \frac{d^3 k'}{\left(\frac{(\mathbf{k}' + \mathbf{q})^2}{2m} - E'\right) \left(\frac{\mathbf{k}'^2}{2m} - E\right) |\mathbf{k}'|} + \int \frac{d^3 k}{\left(\frac{(\mathbf{k} - \mathbf{q})^2}{2m} - E\right) \left(\frac{\mathbf{k}^2}{2m} - E'\right) |\mathbf{k}|} \right]. \quad (\text{A.26})$$

The first term corresponds to the contribution of the “left” two-loop diagram in Fig. 8, i.e., with the potential before the interaction with the current $J(\mathbf{q})$, while the second term is represented by the “right” two-loop diagram in Fig. 8. The corresponding double spectral densities have a form very similar to Δ_0 :

$$\Delta_{1L}^{(a)}(k, k', Q) = \frac{\alpha m}{16\pi} \frac{\pi}{2Q} \frac{1}{k} \theta(|k - Q| < k' < k + Q) \theta(0 < k) \theta(0 < k'), \quad \Delta_{1R}^{(a)}(k, k', Q) = \Delta_{1L}^{(a)}(k', k, Q). \quad (\text{A.27})$$

Explicit calculations yield the following double spectral densities of the two contributions to $\Gamma_1^{(b)}$ related to the “left” and “right” two-loop diagrams in Fig. 8:

$$\Delta_{1L}^{(b)}(k, k', Q) = \frac{\alpha m}{32\pi^6} \frac{1}{Qk} \left[\log^2 \left(\left| \frac{k' - Q + k}{k' - Q - k} \right| \right) - \log^2 \left(\left| \frac{k' + Q + k}{k' + Q - k} \right| \right) \right], \quad \Delta_{1R}^{(b)}(k, k', Q) = \Delta_{1L}^{(b)}(k', k, Q). \quad (\text{A.28})$$

At $Q = 0$, $\Gamma_1^{(a)}(T, T', Q = 0)$ satisfies the Ward identity, $\Gamma_1^{(a)}(T, T', Q = 0) = \Pi_1^{(a)}(T + T')$, whereas $\Gamma_1^{(b)}(T, T', Q = 0)$ vanishes: $\Gamma_1^{(b)}(T, T', Q = 0) = 0$. For large Q and $T, T' \neq 0$, $\Gamma_1^{(b)}(T, T', Q)$ assumes a factorizable form (see Eq. (A.25)):

$$\Gamma_1^{(b)}(T, T', Q) \rightarrow \frac{16\pi\alpha m}{Q^4} \Pi_0(T) \Pi_0(T'). \quad (\text{A.29})$$

At the same time, both $\Gamma_0(T, T', Q)$ and $\Gamma_1^{(a)}(T, T', Q)$ are exponentially suppressed for large Q and $T, T' \neq 0$. Hence, $\Gamma_1^{(b)}$ determines the large- Q behaviour of the vertex function.

c. Dual correlator

The dual correlator $\Gamma_{\text{dual}}(T, T', Q)$ is constructed in a standard way, by application of a low-energy cut to the double spectral representation of the perturbative contribution to (A.16):

$$\Gamma_{\text{dual}}(T, T', Q) = \int_0^{k_{\text{eff}}(Q, T)} dk 2k \exp\left(-\frac{k^2}{2m} T\right) \int_0^{k_{\text{eff}}(Q, T')} dk' 2k' \exp\left(-\frac{k'^2}{2m} T'\right) \Delta(z, z', Q) + \Gamma_{\text{power}}(T, T', Q). \quad (\text{A.30})$$

By construction, the dual correlator corresponds to the ground-state contribution $\exp(-E_g T) \exp(-E_g T') R_g F_g(Q)$.

In the LD limit $T = 0$ and $T' = 0$, $\Gamma_{\text{power}}(T, T', Q)$ vanishes and the ground-state form factor $F_g(Q)$ is related to the low-energy part of the perturbative contribution considered above:

$$\int_0^{k_{\text{eff}}(Q)} dk 2k \int_0^{k_{\text{eff}}(Q)} dk' 2k' \Delta(k, k', Q) = F_g(Q) R_g, \quad (\text{A.31})$$

with $\Delta(k, k', Q) = \Delta_0(k, k', Q) + \Delta_{1L}^{(a)}(k, k', Q) + \Delta_{1R}^{(a)}(k, k', Q) + \Delta_{1L}^{(b)}(k, k', Q) + \Delta_{1R}^{(b)}(k, k', Q) + O(\alpha^2)$.

In order to provide the correct normalization $F_g(Q = 0) = 1$ of the elastic form factor $F_g(Q)$, the effective thresholds should be related to each other according to $k_{\text{eff}}(Q = 0) = \bar{k}_{\text{eff}}$; then the form factor is correctly normalized due to the Ward identity (A.18) satisfied by the spectral densities.

-
- [1] V. L. Chernyak and A. R. Zhitnitsky, JETP Lett. **25**, 510 (1977); Sov. J. Nucl. Phys. **31**, 544 (1980); G. P. Lepage and S. J. Brodsky, Phys. Lett. B **87**, 359 (1979); A. V. Efremov and A. V. Radyushkin, Theor. Math. Phys. **42**, 97 (1980); Phys. Lett. B **94**, 245 (1980).
 - [2] S. Brodsky and G. Lepage, Phys. Rev. D **22**, 2157 (1980).
 - [3] N. Isgur and C. H. Llewellyn Smith, Phys. Lett. B **217**, 535 (1989).
 - [4] F. Cardarelli *et al.*, Phys. Lett. B **332**, 1 (1994).
 - [5] V. V. Anisovich, D. I. Melikhov, and V. A. Nikonov, Phys. Rev. D **52**, 5295 (1995); Phys. Rev. D **55**, 2918 (1997). V. V. Anisovich, D. Bugg, D. I. Melikhov, and V. A. Nikonov, Phys. Lett. B **404**, 166 (1997).
 - [6] P. Maris and C. D. Roberts, Phys. Rev. C **58**, 3659 (1998).
 - [7] V. M. Braun, A. Khodjamirian, and M. Maul, Phys. Rev. D **61**, 073004 (2000).
 - [8] V. Braguta, W. Lucha, and D. Melikhov, Phys. Lett. B **661**, 354 (2008).

- [9] S. Adler, Phys. Rev. **177**, 2426 (1969); J. S. Bell and R. Jackiw, Nuovo Cimento **60A**, 47 (1969). See also R. A. Bertlmann, *Anomalies in Quantum Field Theory* (Clarendon, Oxford, U.K., 1996), and references therein.
- [10] S. Adler and B. Bardeen, Phys. Rev. **182**, 1517 (1969).
- [11] S. J. Brodsky and G. F. de Tera mond, Phys. Rev. D **77**, 056007 (2008).
- [12] H. R. Grigoryan and A. V. Radyushkin, Phys. Rev. D **78**, 115008 (2008).
- [13] M. Belička *et al.*, Phys. Rev. C **83**, 028201 (2011).
- [14] A. P. Bakulev, A. V. Pimikov, and N. G. Stefanis, Phys. Rev. D **79**, 093010 (2009).
- [15] C. J. Bebek *et al.*, Phys. Rev. D **17**, 1693 (1978); T. Horn *et al.*, Phys. Rev. Lett. **97**, 192001 (2006); V. Tadevosyan *et al.*, Phys. Rev. C **75**, 055205 (2007); G. M. Huber *et al.*, Phys. Rev. C **78**, 045203 (2008).
- [16] BABAR Collaboration, B. Aubert *et al.*, Phys. Rev. D **80**, 052002 (2009).
- [17] V. A. Nesterenko and A. V. Radyushkin, Phys. Lett. B **115**, 410 (1982).
- [18] A. V. Radyushkin, Acta Phys. Polon. B **26**, 2067 (1995).
- [19] M. Shifman, A. Vainshtein, and V. Zakharov, Nucl. Phys. B **147**, 385 (1979).
- [20] J. Horejsi and O. Teryaev, Z. Phys. C **65**, 691 (1995).
- [21] D. Melikhov, Phys. Rev. D **53**, 2460 (1996); Phys. Lett. B **380**, 363 (1996); Eur. Phys. J. direct C **4**, 2 (2002) [[arXiv:hep-ph/0110087](#)].
- [22] D. Melikhov and B. Stech, Phys. Rev. Lett. **88**, 151601 (2002).
- [23] V. Braguta and A. Onishchenko, Phys. Lett. B **591**, 267 (2004).
- [24] F. Jegerlehner and O. V. Tarasov, Phys. Lett. B **639**, 299 (2006); R. Pasechnik and O. Teryaev, Phys. Rev. D **73**, 034017 (2006).
- [25] W. Lucha and D. Melikhov, Phys. Rev. D **73**, 054009 (2006); Phys. Atom. Nucl. **70**, 891 (2007). W. Lucha, D. Melikhov, and S. Simula, Phys. Rev. D **76**, 036002 (2007); Phys. Lett. B **657**, 148 (2007); Phys. Atom. Nucl. **71**, 1461 (2008); Phys. Lett. B **671**, 445 (2009). D. Melikhov, Phys. Lett. B **671**, 450 (2009).
- [26] W. Lucha, D. Melikhov, and S. Simula, Phys. Rev. D **79**, 096011 (2009); J. Phys. G **37**, 035003 (2010); Phys. Lett. B **687**, 48 (2010); Phys. Atom. Nucl. **73**, 1770 (2010); J. Phys. G **38**, 105002 (2011); Phys. Lett. B **701**, 82 (2011); W. Lucha, D. Melikhov, H. Sazdjian, and S. Simula, Phys. Rev. D **80**, 114028 (2009).
- [27] V. A. Novikov *et al.*, Phys. Rep. **41**, 1 (1978); M. B. Voloshin, Nucl. Phys. B **154**, 365 (1979); J. S. Bell and R. Bertlmann, Nucl. Phys. B **177**, 218 (1981); Nucl. Phys. B **187**, 285 (1981); V. A. Novikov *et al.*, Nucl. Phys. B **191**, 301 (1981).
- [28] A. Le Yaouanc *et al.*, Phys. Rev. D **62**, 074007 (2000); Phys. Lett. B **488**, 153 (2000); Phys. Lett. B **517**, 135 (2001).
- [29] D. Melikhov and S. Simula, Phys. Rev. D **62**, 074012 (2000).
- [30] B. L. Ioffe and A. V. Smilga, Phys. Lett. B **114**, 353 (1982).
- [31] A. P. Bakulev and A. V. Radyushkin, Phys. Lett. B **271**, 223 (1991).
- [32] V. L. Chernyak, Nucl. Phys. B (Proc. Suppl.) **162**, 161 (2006) [[arXiv:hep-ph/0605327](#)].
- [33] W. Lucha and D. Melikhov, J. Phys. G **39**, 045003 (2012) [[arXiv:1110.2080](#)].
- [34] A. D. Dolgov and V. I. Zakharov, Nucl. Phys. B **27**, 525 (1971); V. I. Zakharov, Phys. Rev. D **42**, 1208 (1990).
- [35] B. L. Ioffe, Int. J. Mod. Phys. A **21**, 6249 (2006).
- [36] S. S. Agaev, V. M. Braun, N. Offen, and F. A. Porkert, Phys. Rev. D **83**, 054020 (2011).
- [37] A.P. Bakulev, S.V. Mikhailov, A.V. Pimikov, and N.G. Stefanis, Phys. Rev. D **84**, 034014 (2011); [arXiv:1202.1781 \[hep-ph\]](#).
- [38] S. Brodsky and G. Lepage, Adv. Ser. Direct. High Energy Phys. **5**, 93 (1989).
- [39] I. Balakireva, W. Lucha, and D. Melikhov, [arXiv:1103.3781 \[hep-ph\]](#).
- [40] T. Feldmann, P. Kroll, and B. Stech, Phys. Rev. D **58**, 114006 (1998); Phys. Lett. B **449**, 339 (1999).
- [41] V. Chernyak, [arXiv:0912.0623 \[hep-ph\]](#).
- [42] Ya. Klopot, A. Oganessian, and O. Teryaev, Phys. Lett. B **695**, 130 (2011); Phys. Rev. D **84** 051901 (2011); JETP Lett. **94**, 729 (2011).
- [43] A. A. Anselm and A. A. Johansen, JETP Lett. **49**, 214 (1989) [*Pisma Zh.Eksp.Teor.Fiz.* **49**, 185 (1989)].
- [44] CELLO Collaboration, H. J. Behrend *et al.*, Z. Phys. C **49**, 401 (1991); CLEO Collaboration, J. Gronberg *et al.*, Phys. Rev. D **57**, 33 (1998).
- [45] BABAR Collaboration, P. del Amo Sanchez *et al.*, Phys. Rev. D **84**, 052001 (2011).
- [46] H. L. L. Roberts *et al.*, Phys. Rev. C **82**, 065202 (2010).
- [47] S. Brodsky, F.-G. Cao, and G. de Tera mond, Phys. Rev. D **84**, 033001 (2011); Phys. Rev. D **84**, 075012 (2011).
- [48] A. Dorokhov, JETP Lett. **91**, 163 (2010).
- [49] P. Kroll, Eur.Phys. J. C **71**, 1623 (2011).
- [50] I. Balakireva, W. Lucha, and D. Melikhov, Phys. Rev. D **85**, 036006 (2012).
- [51] C.-C. Lih and C.-Q. Geng, Phys. Rev. C **85**, 018201 (2012).
- [52] H. Czyz, S. Ivashyn, A. Kor chin, and O. Shekhovtsova, [arXiv:1202.1171](#).
- [53] D. McKeen, M. Pospelov, and J. M. Roney, [arXiv:1112.2207 \[hep-ph\]](#).
- [54] D. Melikhov and B. Stech, [arXiv:1202.4471 \[hep-ph\]](#).
- [55] M. B. Voloshin, Int. J. Mod. Phys. A **10**, 2865 (1995).